

# A modified control method for bi-directional Z-source converters

Wenzheng Xu<sup>1</sup>, *Student Member IEEE*, K.W. Chan<sup>2</sup> Nelson H.L. Chan<sup>3</sup> Junwei Liu<sup>4</sup>  
<sup>1,2,3,4</sup> Department of Electrical Engineering, The Hong Kong Polytechnic University, Hong Kong  
<sup>1</sup> E-mail: wen-zheng.xu@connect.polyu.hk

**Abstract**—This paper proposes a new “ $\alpha\beta$ ” control method modified from traditional SPWM in a basic bi-directional DC-DC Z-source converter topology which are expected to be applied in Electric Vehicle’s charging and discharging. The converter can both boost and reduce the voltage in the operation of battery’s discharging to the grid with this closed loop control scheme. It can also achieve charging the battery from the grid with special control of switches. PID control is adopted to improve the overall performance. Simulation results in Matlab Simulink proved the effectiveness of this control method applied on this bi-directional topology.

**Keywords**—Z-source inverter, modified SPWM control, shoot-through state inserting, bi-directional EV charging.

## I. INTRODUCTION

Z-Source topology is proposed by prof. Peng F.Z. in 2003 [1] which can be adopted in either current source inverters or voltage source inverters. It is a special L-C impedance network and usually connects the power source and conversion topologies. With the existence the Z-source topology, it can provide voltage boost/buck properties and solve the shoot-through problem of inverter’s bridges, which can’t be achieved by traditional inverters because the two switches in one bridge can’t be turned on simultaneously without the unique L-C impedance network. Because these features of the Z-source topology, this paper tries to adopt this topology in the discharging and charging of Electric Vehicles (EVs). Rated voltage of EVs is different but the voltage of the grid is constant, so the Z-source topology based converter is expected to reduce or boost voltage in different conditions.

In the last ten years researchers have studied a lot about the Z-source topology, including updated version of semi-Z-source inverter [2]. The benefits of the topology are clear and researchers are also trying to overcome the limitations such as high voltage rating for certain devices and discontinuous input current [3] [4]. Other limitations include Z-source inverter has lower average switching device power in low boost ratio range [5] and harmonics current in three-phase inverter [6].

Z-source topology based converter has been studied in difference fields. Several single-stage single-phase non-isolated semi-Z-source inverters are proposed which are

especially suitable for a PV panel in low-voltage grid-connected application as a low-cost micro inverter [7]. The control of full-cell based Z-source converter also shows good performance under a well-designed calculation methodology [8] [9]. Driving a motor is also applicable for this Z-source topology based converter which extended the voltage range as well as reduced line harmonics [10].

This paper proposes a new “ $\alpha\beta$ ” PWM control scheme for single-phase Z-source inverters. Detailed analysis and simulation of the control scheme is conducted in platform of MATLAB Simulink. The principle of closed-loop PID control is also represented, which is also different with conventional control schemes for voltage-source inverters. Simulation of open-loop “ $\alpha\beta$ ” control shows the Z-source converter can both boost and reduce voltage depends on the value of  $\alpha$  and  $\beta$ , while the Total Harmonic Distortion (THD) of output voltage increases as the voltage ratio increases. Closed-loop control with PID solves this problem well and THD of output voltage is much lower in the same circumstance. The converter can also work as a rectifier to charge the EV battery. The merits and limitations of the proposed control method is discussed compared with others. It has bright future to be adopted in EV’s charging with isolated topology and more complicated control algorithm.

## II. TOPOLOGY AND PRINCIPLE OF BI-DIRECTIONAL SINGLE-PHASE Z-SOURCE CONVERTER

### 2.1 Topology of single phase Z-source inverter

In most cases the Z-source topology is applied in inverters because of its unique feature. Fig.1 presents a basic topology diagram of un-isolated single-phase voltage-source inverters. The dashed rectangle shows the pair of inductors  $L_1$ ,  $L_2$  and capacitors  $C_1$ ,  $C_2$  which composed the Z-source topology.

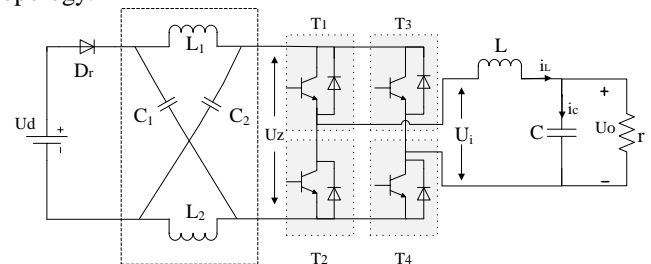


Fig. 1. Topology of an un-isolated Z-source inverter (single phase)

Generally, the inductance of the two capacitors is the same, and the capacitance of the two inductors is also the same. In other word, the Z-source topology is symmetrical. In practical applications an isolating transformer is normally adopted, but the whole circuit is not symmetrical any more. [11] Thus in this paper, research starts from this basic inverter topology firstly.

The right part of this Z-source inverter is a conventional full-bridge inverter. It is formed simply by combining the Z-source topology and the traditional voltage source inverter, whereas a diode  $D_r$  is needed in series with the power source to block the potential reverse flow of current [12]. For other converter or inverter topologies, it is also applicable to connect to the Z-source topology on the primary side, for example Fig.2 shows a three-phase version of Z-source inverter used to charging the motor [11]. Besides the Z-source topology part, all other circuits are commonly used already. Thus, Z-source topology based inverters or converters can be easily formed and widely used.

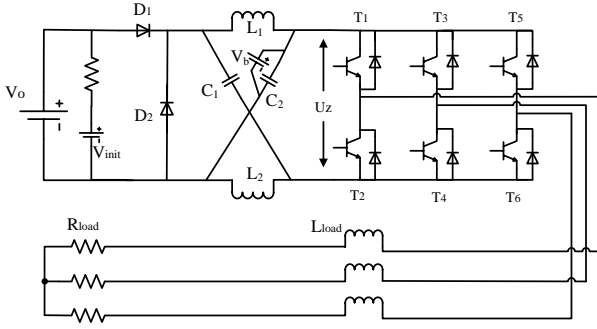


Fig. 2. A three phase Z-source inverter for EV

## 2.2 Principle of voltage boosting properties

For this un-isolated Z-source inverter, the two major limitations for traditional inverter as mentioned before are all well solved. Firstly, with the z-source topology, there is no possibility that the two switches in one bridge are turned on at the same time, since the input DC voltage source can never be short-circuited. Secondly, the Z-source inverters ingeniously take advantage of the shoot-through states to realize the boost function of invention. Simulation in Matlab Simulink has proven that it is easy for a z-source inverter with 150V dc voltage to output nearly 300V ac sinusoidal voltage, while the THD is less than 8%.

Firstly we assume that the capacitance of the two capacitors  $C_1$  and  $C_2$  is  $C$ , and the inductance of the two inductors  $L_1$  and  $L_2$  is  $L$ . Assume that the inverter bridge stays in the shoot-through state for an interval  $T_s$ , in a switching cycle  $T$ . In shoot-through state, the two switches in one certain bridge are simultaneously turned on, thus the voltage across the bridge  $U_z$  is zero. The equivalent circuit is shown as Fig.3. It is obvious that:

$$V_{L1} = V_{L2} = V_{C1} = V_{C2} \quad (1)$$

$$U_{z(s)} = 0 \quad (2)$$

Now assume the total time of inverter's bridge which is in non-shoot-through states is  $T_n$  during one switching cycle  $T$ . The equivalent circuit is shown as Fig. 4. We can get:

$$V_{L1} = V_{L2} = U_d - V_{C1} = U_d - V_{C2} \quad (3)$$

$$U_z = V_C - V_{L1} = V_C - V_{L2} = 2V_C - U_d \quad (4)$$

In steady state, the average voltage of the inductors over one switching period  $T$  should be zero, thus we have:

$$\overline{V_L} = (T_s \cdot V_C + T_n \cdot (U_d - V_C)) / T = 0 \quad (5)$$

One cycle consists of shoot-through state whose total time is  $T_s$  and non-shoot-through state whose total time is  $T_n$ .

$$T = T_s + T_n \quad (6)$$

From (5) and (6), we can get:

$$\frac{V_C}{U_d} = \frac{T_n}{T_n - T_s} \quad (7)$$

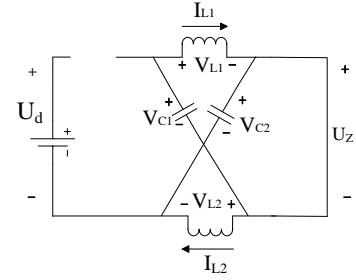


Fig. 3. Equivalent circuit of shoot-through state

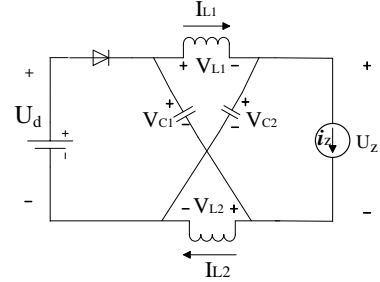


Fig.4 Equivalent circuit of non-shoot-through state

The average dc link voltage across the inverter bridge  $U_z$  can be found as follows:

$$\overline{U_z} = (T_s \cdot 0 + T_n \cdot (2V_C - U_d)) / T = \frac{T_n}{T_n - T_s} U_d = V_C \quad (8)$$

$$\frac{T_n}{T_n - T_s} \geq 1 (T_s \geq 0, T_n > 0) \quad (9)$$

From equation (9) we can learn that the DC input voltage of the traditional inverter part  $U_z$  is larger than  $U_d$ . In this way, the Z-source topology can function as a boost part for a

DC-DC converter. The AC output voltage of Z-source inverter is thus boosted. From Fig.1 we can know that the voltage  $U_i$  changes between  $+U_z$ ,  $-U_z$  and 0. According to (4) and (8), the peak value of  $U_i$  can be derived as:

$$\hat{U}_i = 2V_c - U_d = \left(\frac{2T_n}{T_n - T_s} U_d\right) - U_d = \frac{T}{T_n - T_s} U_d = B \cdot U_d \quad (10)$$

$$B = \frac{T}{T_n - T_s} = \frac{1}{1 - 2T_s/T} \geq 1 \quad (11)$$

In equation (11),  $B$  represents the voltage gain. We define  $\alpha$  as the modulation ratio of magnitude of regulation wave and of carrier wave, then the output AC voltage of Z-source inverters can be given by:

$$v_{ac} = \alpha \cdot B \cdot \frac{1}{2} V_d = \frac{BV_d \hat{V}_{regulation}}{\hat{V}_{carrier}} \quad (12)$$

In total, with the implementation of shoot-through state, dc side voltage  $U_d$  is boosted to  $U_z$  by the Z-source topology, thus the AC output voltage is larger than the original DC side voltage.

### 2.3 The “ $\alpha \times \beta$ ” PWM control scheme of Single-phase Z-source inverters

Since the proposal of Z-source inverters, many researchers have proposed different PWM control strategies. It is believed that most of the original PWM control schemes can be modified to adopt the new Z-source inverters [12]. Principally, the control scheme for Z-source inverters is to insert the shoot-through states appropriately based on original ones. The “ $\alpha \times \beta$ ” PWM control strategy in this paper is based on SPWM (Sinusoidal Pulse Width Modulation) of traditional inverters.

From the perspective of strategies for Z-source topology, the proposed “ $\alpha \times \beta$ ” PWM strategy for Z-source inverters belongs to simple boost control [12] with minor modification. Fig.5 shows the signals of four switches of a conventional voltage source inverter with SPWM control. The goal of the strategies is to insert shoot-through states in an appropriate way, and the method is to modify the modulation wave of one bridge to allow time slots when both the two switches are turned on.

Signals of the switches

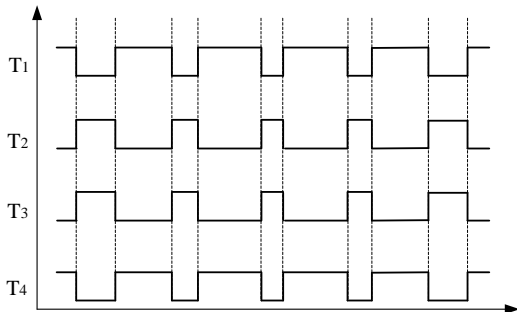


Fig. 5. Signals of the four switches of voltage-source inverter

As shown in Fig.6, the black curve represents modulation wave to generate signal for  $T_1$  and  $T_2$ . When the value of modulation wave is larger than that of the carrier wave,  $T_1$  is turned on and  $T_2$  is turned off, and vice versa. Assume the magnitude of modulation wave is  $\alpha$ , then we set  $\alpha \times \beta$  as the magnitude of modified wave. In the positive half cycle,  $\beta$  is a constant less 1, represented by  $\beta_1$ , for example 0.8, while in the negative half cycle,  $\beta$  is a constant more than 1, represented as  $\beta_2$ , for example 1.25. In the positive half cycle, the magnitude of modified wave is less than original wave since  $\alpha > 0$  and  $\beta < 1$ , while in the negative half cycle the magnitude of modified wave is still less than original one since  $\alpha < 0$  and  $\beta > 1$ .

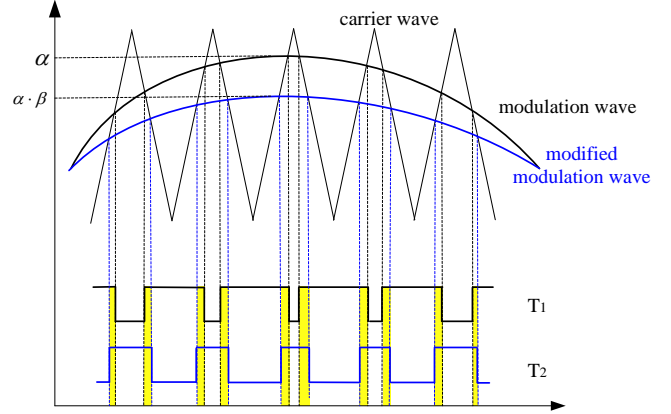


Fig. 6. Strategy to insert shoot-through states I

Signals of the switches

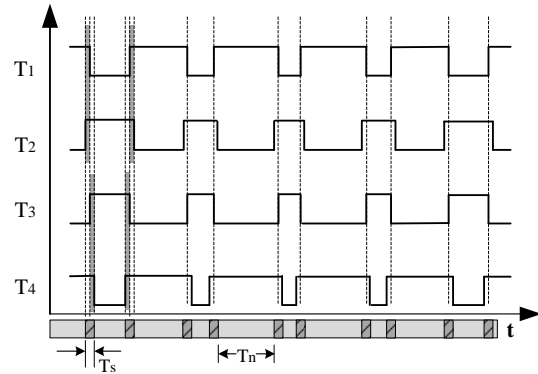


Fig. 7. T signals generated by inserting the shoot-through states

In this way, the absolute value of modified modulation wave is always lower than the original one except the zero points. As Fig. 6 shows, the signal of  $T_2$  is different from original one. There are many time slots that  $T_1$  and  $T_2$  are turned on simultaneously, as the yellow shadow part shows. Shoot-through states are inserted and distributed all over the cycle just like that appears in Fig 7. Though waveforms of the positive and negative half cycle are not exactly the same shape, the whole PWM scheme is still symmetric because the two bridges complement each other. For example, the waveforms of  $T_1$  &  $T_2$  in the positive half cycle are the same with waveforms of  $T_3$  &  $T_4$  in the negative half cycle. Thus the

whole system is still symmetric and stable. For closed-loop control, the value of  $\beta$  keeps changing according to the feedback of relevant data and processed by DSP controller. Considering the switches can't support too large switching frequency, the DSP will guarantee that switching frequency is less than 20kHz, which is designed for most popular IGBTs.

In total,  $\alpha$  determines the basic voltage ratio of output voltage versus DC input voltage, and  $\beta$  affects the time of shoot-through states in one cycle which can boost voltage.

#### 2.4 Topology of bi-directional Z-source converters

Researchers have found that for single-phase Z-source inverters, the reverse power flow from the grid back to the dc side can be achieved by connecting a switch such as IGBT with an anti-reverse diode [13], and this paper also adopts the proposed topology. Fig. 8 shows the topology of bi-directional Z-source converter, and  $T_5$  represents the IGBT and the diode.

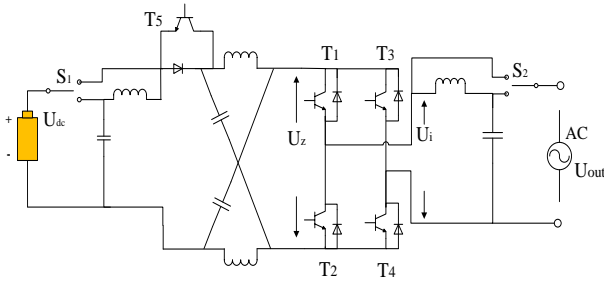


Fig.8 Topology of bi-directional Z-source converters

Ref. [13] describes how such a bi-directional Z-Source inverter can be designed and controlled to facilitate power flow in both directions. The switching signal of this additional IGBT is derived so that its presence would not affect the voltage buck/boost ratio [13]. The methods to generate switching signals for the new IGBT as well as those in the conventional VSI are also described for the simple-boost control in Ref. [12]. It can be easily modified for any other switching strategy. Fig.9 shows the power flow path when the power flows from the DC side (battery) to AC side (grid). In this case, the converter is operating in inverter mode. Fig.10 shows the power flow path when the power flows from the AC side (grid) to DC side (battery). In this case, the converter is operating in rectifier mode, and the battery is being charged. Reactive power compensation is also considered with method provided in Ref. [14] and Ref. [15] based on PHEV bi-directional charger.

The two switches  $S_1$  and  $S_2$  are implemented at the two sides of the Z-source converter respectively. The two switches can be relays or manual STDP switches. There are two LC filters in this topology. Filter composed by  $L_2$  and  $C_2$  is used at the AC side when the converter works in the

inverter mode. Filter composed by  $L_1$  and  $C_1$  is used at the DC side when the converter works in the rectifier mode.

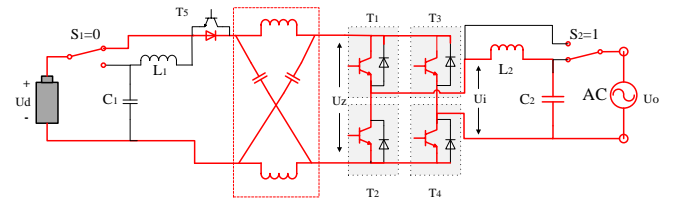


Fig.9: Power flow of single-phase bi-directional Z-source converters (DC to AC)

In inverter mode, IGBT  $T_5$  is not conducted while the diode is carrying current from battery to the grid. Power flow is represented with red line in Fig.9. Switch  $S_1$  is turned off, i.e. the LC filter at the dc side is not connected to the converter. Switch  $S_2$  is turned on, i.e. the LC filter at the ac side is connected to the converter. In this case, the topology is exactly the same as single-phase Z-source inverter represented before.

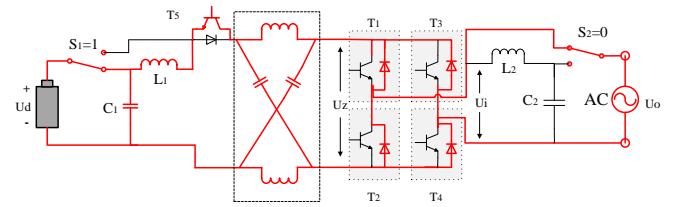


Fig. 10. Power flow of single-phase bi-directional Z-source converter (AC to DC)

In rectifier mode, the IGBT  $T_5$  is conducted. Power flow is represented with red line in Fig.10. Switch  $S_1$  is turned on, i.e. the LC filter at the dc side is connected to the converter, which helps to regulate the dc output voltage. Switch  $S_2$  is turned off, i.e. the LC filter at the ac side is not connected to the converter. In this case, the four diodes paralleled with  $T_1$ ,  $T_2$ ,  $T_3$  and  $T_4$  work as a rectifier bridge, while the four switches are not conducted.

### III. SIMULATION OF BI-DIRECTIONAL Z-SOURCE CONVERTER

#### 3.1 Open-loop operation of the “ $\alpha \times \beta$ ” PWM control scheme

Simulation of the proposed bi-directional Z-source converter controlled by “ $\alpha \times \beta$ ” PWM scheme is conducted in Matlab Simulink. Fig.11 shows the open-loop PWM generation strategy. Since  $\beta$  is changed in different half cycles, we use square wave model to modify the value of  $\beta$ . The four signals generated at output 1-4 represents control signals for the switches  $T_1$  to  $T_4$  respectively. Fig 12 shows the generated modulation waves where black curve is “ $\alpha$ ” and red curve is the modified “ $\alpha \times \beta$ ”. As the red curve is always lower than the black curve except zero points, shoot-through states are inserted throughout the operation. Shoot-through states are more distributed in the peak or valley area

of the modulation wave, thus the output voltage presents a character that the waveform shape is sharp at peak or valley area but smooth in the middle area.

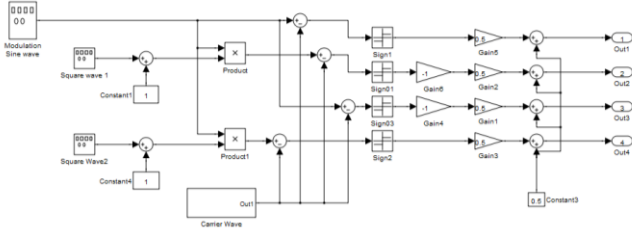


Fig.11 The “ $\alpha \times \beta$ ” PWM generation strategy in Simulink.

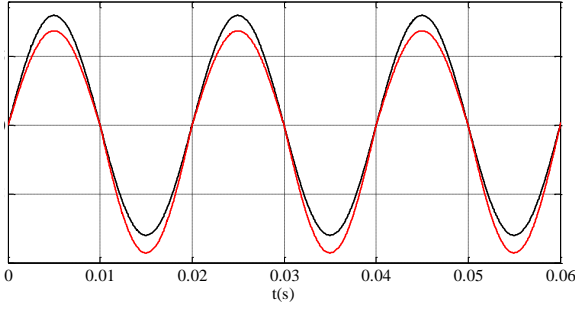


Fig. 12. Modulation waves generated by “ $\alpha \times \beta$ ” PWM scheme

Detailed parameters of the circuit are:  $L_1=L_2=800\mu\text{H}$ ,  $C_1=C_2=3.3\text{mF}$ , the DC side voltage  $U_d=200\text{V}$ ,  $L=1\text{mH}$ ,  $C=2\text{mF}$ . Simulation results are shown in the table 1. It is obvious that output voltage value is boosted with more differential between the original and modified modulation wave, while the THD increases as well. The parameters of inductors and capacitors also have great influence on the THD, however when  $\beta_1$  is smaller than 0.8, the THD of output waveform is normally larger than 10%, which is not acceptable for practical use.

Table 1: Simulation results of open-loop  $\alpha \times \beta$  PWM scheme

DC voltage/V	$\alpha$	$\beta$		$V_{\text{peak}}/\text{V}$	THD
		$\beta_1$	$\beta_2$		
200	0.75	0.94	1.063	211.8	2.55%
200	0.75	0.90	1.111	254.6	4.94%
200	0.75	0.85	1.315	273.1	7.19%
200	0.75	0.82	1.219	296.4	8.28%

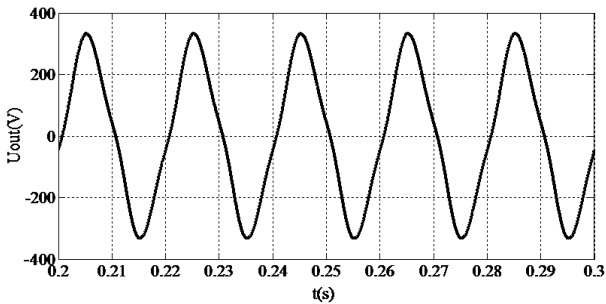


Fig 13. Output voltage waveform when  $\beta_1=0.70$  and  $\beta_2=1.42$

When we set a higher  $U_{\text{ref}}$  in control, which is much higher than the DC side voltage, the controller has to insert lots of shoot-through states to boost the voltage. However, the THD of the output waveform is affected then. Fig. 13 shows the output voltage waveform when  $\beta_1=0.70$  and  $\beta_2=1.42$ .

### 3.2 Closed-loop operation of the “ $\alpha \times \beta$ ” PWM control scheme for the Z-source inverter

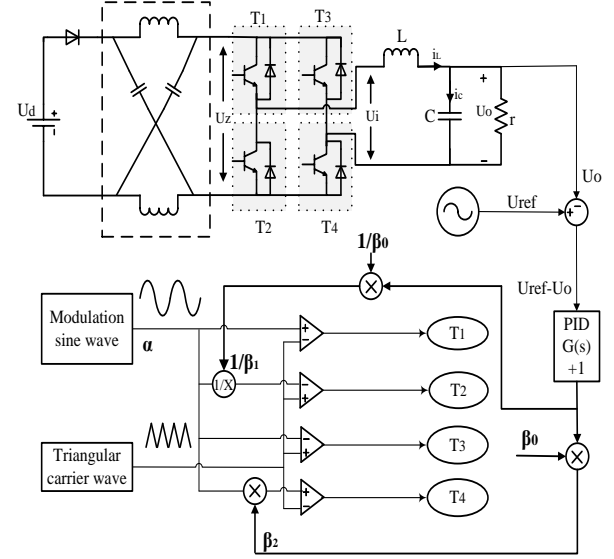


Fig 14. Diagram of closed-loop PID control of Z-source inverters

For closed-loop PID control of Z-source inverters, when  $\beta$  increases, the output voltage of Z-source inverter and the boost ratio also increase, since the duty of shoot-through time is in positive correlation with the value of  $\beta$ . In closed-loop PID control, “ $\alpha$ ” is a constant, while “ $\beta$ ” is generally given by:

$$\beta = \beta_0 \times (1 + G(s)(U_{\text{ref}} - U_o)) \quad (13)$$

$G(s)$  represents the PID function block [16], and  $U_{\text{ref}}$  represents the ideal output voltage of the Z-source inverter when  $\beta=\beta_0$ . The above equation shows the basic methodology of determining  $\beta$ . In the positive and negative half cycle, the value of  $\beta$  is different as discussed before, marked as  $\beta_1$  and  $\beta_2$  respectively. When the output voltage value is larger than the expected one,  $U_{\text{ref}} - U_o$  becomes negative, then  $\beta_1$  becomes larger and  $\beta_2$  becomes smaller.

Table 2: Simulation results of closed-loop  $\alpha \times \beta$  PWM scheme

DC voltage/V	$\alpha$	$\beta$		$V_{\text{peak}}/\text{V}$	THD
		$\beta_0$	$B_{\text{p-p}}$		
300	0.8	0.850	0.042	305.9	2.00%
300	0.8	0.875	0.042	344.9	2.86%
300	0.8	0.900	0.045	378.4	3.77%
300	0.8	0.925	0.044	401.0	5.08%

According to Fig. 6, less shoot-through states are inserted thus the boosted voltage would reduce to match the reference voltage. In this way, stable output is guaranteed when disturbance occurs and output is controlled. Dynamic performance can be enhanced by adjusting  $G(s)$ .

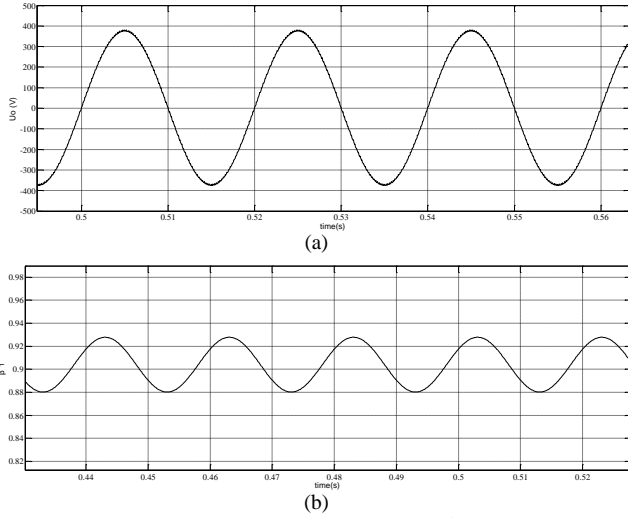


Fig.15. (a) Output voltage of Z-source inverter of  $\alpha \times \beta$  PWM scheme when  $\beta_1=0.9$ ,  $\beta_2=1.11$  (b) The value of  $\beta$  in simulation

The parameters for simulation is the same as open-loop one, and shows same result as shown in Fig.15 (a). We can also see the  $\beta$  varies in a sinusoidal way in operation in Fig.15 (b). Compared to Table 1, the simulation result in Table 2 shows better THD performance because of the varying  $\beta$  overcomes the problem that shoot-through states are more inserted in the peak and less inserted in the valley when  $\beta$  is constant.

#### IV. SIMULATION OF BI-DIRECTIONAL Z-SOURCE CONVERTER

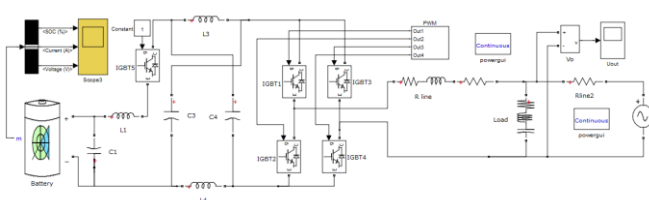


Fig.16. Diagram of bi-directional Z-source converter in Simulink

To test the bi-directional power flow of the Z-source converter, simulation of Fig.16 is conducted. The battery model in simulink represents the integrated battery pack. The battery type is Lithium-ion, and rated voltage is 130V. The *r.m.s.* value of AC power source is 220V.

For the battery's charging, i.e. AC do DC of the converter, the initial SOC (State of Charge) of the battery is set as 10%. Simulation result is shown in Fig.17 and we can see the charging current is stable at 14.6A while the actual voltage of the battery keeps increasing. The Z-source topology does not play a significant role in the process,

while the L-C filter of  $L_1$  and  $C_1$  in Fig.16 helps to stabilize the output DC current after the diode rectifier.

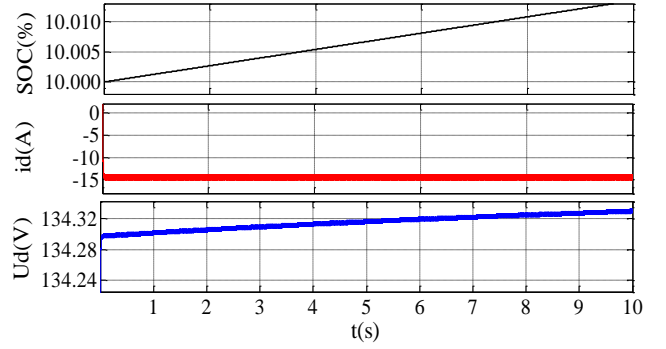


Fig.17. Charging of the EV battery

For the battery's discharging, i.e. DC do AC of the converter, the initial SOC (State of Charge) of the battery is set as 100%. Simulation result is shown in Fig.18. The

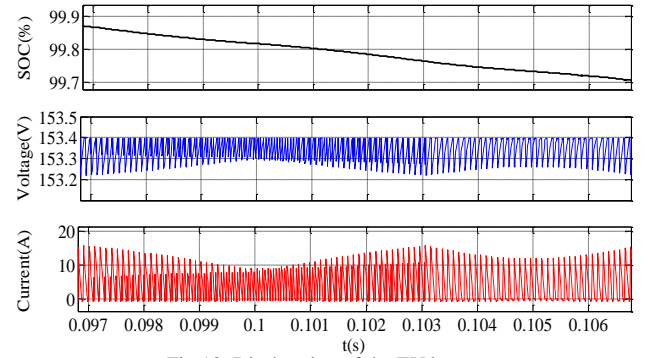


Fig.18. Discharging of the EV battery

In conclusion, simulation of both the open-loop and closed loop " $\alpha \times \beta$ " PWM control of the Z-source shows satisfying performance, and both DC to AC and AC to DC power flow is feasible. It is easy to adopt and the THD of closed-loop is lower than some existing ones based on squarewave modulation, with good voltage-boosting effects. However, the asymmetric feature of modulation waves in the positive and negative half cycles slightly affects the symmetry of output voltage. For applications in three-phase inverters, control schemes based on space vector pulse width modulation may perform better. Further study and improvement of this control scheme is desired.

#### V. CONCLUSION AND FUTURE WORK

In this paper, a new closed-loop " $\alpha \times \beta$ " control scheme based on SPWM for bi-directional Z-source converters is proposed. Simulation results in Matlab Simulink show that the new control method applied on the bi-directional Z-source DC-DC converter is effective and the performance of both charging and discharging are basically satisfying. Simulation of open-loop " $\alpha \times \beta$ " control shows the Z-source

converter can both boost and reduce voltage depending on the value of  $\alpha$  and  $\beta$ , while the THD of output voltage increases as the voltage ratio increases. Closed-loop control with PID solves this problem well and THD of output voltage is much lower in the same circumstance. The principle of charging the battery is a diode rectifier bridge, and it is not significantly affected by the Z-source topology.

The limitation of this converter is that the power level of battery's discharging is relatively lower thus fast-discharging can't be achieved well. When the output AC voltage of the converter is much higher than DC input voltage, the THD of output voltage becomes higher too. In practical operation, the inductors might become hot because of the high switching frequency so the operation time or the inductor size is relatively limited. Future work contains a well-isolated topology, improvement of overall power level and efficiency, more flexible application, and more scientific control algorithm. A hardware platform is built and being tested to demonstrate the feasibility and stability. With its advantage of shoot-through states and flexible voltage boosting, the Z-source converter can contribute more in the V2G system.

#### REFERENCES

- [1] Peng F. Z., "Z-source inverter", IEEE Transactions on Industry Applications, vol. 39, no. 2, pp. 504-510, 2003.
- [2] Cao D., Jiang S., Yu X., "Low-cost semi-Z-source inverter for single-phase photovoltaic systems", IEEE Transactions on Power Electronics, vol. 26, no. 12, pp. 3514-3523, 2011.
- [3] Peng F. Z., Shen M., Qian Z., "Maximum boost control of the Z-source inverter", IEEE Transactions on Power Electronics, vol. 20, no. 4, pp. 833-838, 2005.
- [4] Anderson J., Peng F. Z., "Four quasi-Z-Source inverters", Power Electronics Specialists Conference 2008, IEEE, pp. 2743-2749, 2008.
- [5] Florescu A., Stocklosa O., Teodorescu M., "The advantages, limitations and disadvantages of Z-source inverter", International Semiconductor Conference, IEEE, vol. 2, pp. 483-486, 2010.
- [6] Gao F., Loh P. C., Blaabjerg F., "Operational analysis and comparative evaluation of embedded Z-source inverters", Power Electronics Specialists Conference 2008, IEEE, pp. 2757-2763, 2008.
- [7] Cao D., Jiang S., Yu X., "Low-cost semi-Z-source inverter for single-phase photovoltaic systems", IEEE Transactions on Power Electronics, vol. 26, no. 12, pp. 3514-3523, 2011.
- [8] Jung J. W., Keyhani A., "Control of a fuel cell based Z-source converter", IEEE Transactions on Energy Conversion, vol. 22, no. 2, pp. 467-476, 2007.
- [9] Peng F. Z., Shen M., Holland K., "Application of Z-source inverter for traction drive of fuel cell - battery hybrid electric vehicles", IEEE Transactions on Power Electronics, vol. 22, no. 3, pp. 1054-1061, 2007.
- [10] Peng F. Z., Yuan X., Fang X., "Z-source inverter for adjustable speed drives", Power Electronics Letters, IEEE, vol. 1, no. 2, pp. 33-35, 2003.
- [11] Carli G., Williamson S. S. Technical considerations on power conversion for electric and plug-in hybrid electric vehicle battery charging in photovoltaic installations. Power Electronics, IEEE Transactions on, 2013, 28(12): 5784-5792.
- [12] Loh P. C., Vilathgamuwa D. M., Lai Y. S., "Pulse-width modulation of Z-source inverters", IEEE Transactions on Power Electronics, vol. 20, no. 6, pp. 1346-1355, 2005.
- [13] Rajakaruna S., Zhang B., "Design and control of a bidirectional Z-Source inverter", Power Engineering Conference 2009, IEEE, pp. 1-6, 2009. pp. 2176-2183.
- [14] Kisacikoglu M. C., Ozpineci B., Tolbert L. M., "Examination of a PHEV bidirectional charger system for V2G reactive power compensation", Applied Power Electronics Conference and Exposition, 2010 Twenty-Fifth Annual IEEE, pp. 458-465, 2010.
- [15] Kisacikoglu M. C., Ozpineci B., Tolbert L. M., "Single-phase inverter design for V2G reactive power compensation", Applied Power Electronics Conference and Exposition, 2011 Twenty-Sixth Annual IEEE, pp. 808-814, 2011.
- [16] Visioli A., *Practical PID control*, Springer-Verlag London Limited, 2006.